Available online at www.sciencedirect.com
ScienceDirect
Trans. Nonferrous Met. Soc. China 24(2014) 3785−3791
Transactions of Nonferrous Metals Society of China
www.tnmsc.cn

Microstructure and tribological behavior of Mg−Gd−Zn−Zr alloy with LPSO structure

Li-jie CAO[1], Yu-juan WU[2], Li-ming PENG[2,3], Qu-dong WANG[2,3], Wen-jiang DING[2,3]

1. College of Mechanical Engineering, Shanghai University of Engineering Science, Shanghai 201600, China;
2. National Engineering Research Center of Light Alloy Net Forming, Shanghai Jiao Tong University, Shanghai 200240, China;
3. State Key Laboratory of Metal Matrix Composites, Shanghai Jiao Tong University, Shanghai 200240, China

Received 17 October 2013; accepted 10 November 2014

Abstract: A Mg−14.28Gd−2.44Zn−0.54Zr (mass fraction, %) alloy was prepared by conventional ingot metallurgy (I/M). The microstructure differences in as-cast and solution-treated alloys were investigated. Sliding tribological behaviors of the as-cast and solution-treated alloys were investigated under oil lubricant condition by pin-on-disc configuration. The wear loss and friction coefficients were measured at a load of 40 N and sliding speeds of 30−300 mm/s with a sliding distance of 5000 m at room temperature. The results show that the as-cast alloy is mainly composed of α-Mg solid solution, the lamellar 14H-type long period stacking ordered (LPSO) structure within matrix, and β-[$(Mg,Zn)_3Gd$] phase. However, most of the β-phase transforms to X-phase with 14H-type LPSO structure after solution heat treatment at 773 K for 35 h (T4). The solution-treated alloy presents low wear-resistance, because the hard β-phase is converted into thermally-stable, ductile and soft X-$Mg_{12}GdZn$ phase with LPSO structure in the alloy.

Key words: Mg−Gd−Zn−Zr alloy; long period stacking ordered (LPSO) structure; microstructure; friction; wear

1 Introduction

Magnesium alloys have been attractive as the lightest structural components in automotive industry with a growing trend toward reducing energy consumption and air pollution, due to their attractive properties such as low density, high specific strength, ease of recycling and better vibration-damping capacity [1,2]. However, the poor wear performance and corrosion resistance of Mg alloy greatly limit its wide structural applications [3,4]. A number of techniques have been developed to improve the wear resistance (WR) of Mg alloys such as laser surface melting treatment and ultrasonic nanocrystalline surface modification (UNSM) [5,6] and cryogenic treatment (CT) [7].

At present, rare earth magnesium alloys have been developed for its high strength, high temperature resistance and creep resistance, which offer alternative candidate for applications in aerospace and automotive industries. Mg−RE−Zn alloys have attracted more and more attention because of solid solution strengthening, aging strengthening and the formation of long period stacking ordered (LPSO) structure [8−18]. LPSO structures can act as hardening phases, which will improve comprehensive mechanical properties in Mg−RE−Zn alloys [8−11]. Published reports on the friction and wear behaviors of Mg−RE−Zn alloy are quite limited. AN et al [19] performed dry sliding tests on as-cast Mg−Zn−2Y alloys using a pin-on-disc configuration. Their results revealed that Mg−Zn−2Y exhibited good wear resistance compared with AZ91 for applied loads in excess of 80 N. ZHANG et al [20] investigated the dry sliding wear of as-cast Mg−Zn−Y alloy using block-on-wheel system. They revealed that the Mg−Zn−Y quasicrystal materials exhibited the lowest friction coefficients and the best wear resistance at all applied loads when the Y content was 2% (mole fraction). LIU et al [7] investigated the wear behavior of Mg−

Foundation item: Projects (51304135, 50971089) supported by the National Natural Science Foundation of China; Project (A1420110045) supported by National Defense Basic Research Plan, China; Project (11QH1401200) supported by the Shanghai Phospherus Program, China; Project (NCET-11-0329) supported by the New Century Excellent Talents in University of Ministry of Education of China

Corresponding authors: Li-jie CAO; Tel: +86-21-67791193; E-mail: clj@sues.edu.cn

DOI: 10.1016/S1003-6326(14)63533-0

1.5Zn−0.15Gd alloy before and after cryogenic treatment (CT) by dry sliding wear test. Their experimental results showed that the wear resistance of the alloys has been significantly improved after CT. HU et al [17] conducted dry sliding tests on as-cast and cast+T6 Mg−11Y−5Gd−2Zn alloy using a ball-on-plate configuration. They revealed that the wear rate of as-cast alloy is higher than that of cast+T6 alloy. CAO et al [18] investigated the sliding friction and wear behaviors of Mg−11Y−5Gd−2Zn−0.5Zr (mass fraction, %) alloy were investigated under oil lubricant condition by pin-on-disk configuration. Test results indicated that the hard and thermally stable Mg_{12}(Y,Gd)Zn phase with long-period stacking ordered structure in the alloy presented significant wear resistance. But so far the friction and wear behaviors of Mg−Gd−Zn−Zr alloys with LPSO structure have not yet been reported.

In the present work, a Mg−14.28Gd−2.44Zn−0.54Zr alloy was produced by conventional ingot metallurgy (I/M) technique. The effect of solid solution treatment on the as-cast microstructures, especially the lamellar 14H-type LPSO structure, mechanical properties and tribological behaviors were studied in I/M and DC alloys.

2 Experimental

The alloy used in this work was Mg−14.28Gd−2.44Zn−0.54Zr (mass fraction, %). Firstly, pure Mg was melted in an electric resistance furnace with a mild steel crucible under a protective gas (0.3% SF_6 and 99.7% CO_2, volume fraction). Secondly, pure Zn metal and Mg−25Gd (mass fraction, %) were melted at about 973 K. Thirdly, Mg−30Zr (mass fraction, %) was added into the melt at about 1053 K. Finally, the melt was poured at about 1023 K into the mild steel mold preheated to 473 K. The alloy ingots were cooled in air, and cut into small specimens by electric spark linear cutting. The specimens were solution-treated at 772 K for 35 h in a SX2-8-10-type high-temperature heat treatment furnace and then immediately quenched in cold water. Actual chemical compositions of these alloys were determined by an inductively coupled plasma analyzer (PerkinElmer, Plasma 400).

Sliding wear tests were carried out in a pin-on-disc wear testing apparatus (model: MMW−1A, multi-functional vertical friction and wear tester) under varying sliding speeds at a fixed applied load of 40 N. The Mg alloy cylindrical pin specimens were 32 mm in length and 10 mm in diameter. A reciprocating grey cast iron plate of dimensions 60 mm×150 mm×10 mm with a hardness of HB 210 was counterpart. The stroke length was 80 mm. The contact surfaces were lubricated with synthetic engine oil (15W/40SG). The wear loss and friction coefficients were measured with a constant sliding distance of 5000 m at room temperature.

The specimens for microstructures analyses, etched by 4% HNO_3 and 96% ethanol, were observed by the Zeiss reversal optical microscope (OM, Axio Observer A1) and a scanning electron microscope (SEM, FEI SIRION 200) at 5−20 kV equipped with an Oxford energy disperse X-ray spectrometer (EDS).

Tensile tests at room temperature were carried out using a Zwick T1-FR020TN A50-type electronic universal testing machine at a strain rate of 1.67×10^{-3} s^{-1}. Moreover, Vickers hardness tests were measured by a HV-30 Vickers hardness tester with a 5 kg load for 30 s.

3 Results and discussion

3.1 Microstructure

3.1.1 Chemical composition

The designed composition of studied alloy was Mg−13.96Gd−2.32Zn−0.6Zr. The actual chemical composition of the alloy was Mg−14.28Gd−2.44Zn−0.54Zr (mass fraction, %). Therefore, the difference between the actual and the designed compositions was little, which satisfied the need.

3.1.2 As-cast microstructure

Figure 1 shows the OM and SEM images of the as-cast Mg−14.28Gd−2.44Zn−0.54Zr alloy. The microstructure of the as-cast alloy is confirmed to be composed of α-Mg matrix, the lamellae and β-phase as secondary eutectic phase [15]. The lamellae within α-Mg matrix have a 14H-LPSO structure, as reported by WU et al [14]. EDS spectrum illustrates that β-phase is $(Mg,Zn)_3Gd$ [14].

3.1.3 Solution-treated microstructure

Figure 2 shows the OM and SEM images of the Mg−14.28Gd−2.44Zn−0.54Zr alloy solution-treated at 773 K for 35 h. It indicates that the lamellae still exist within matrix. Moreover, a novel lamellar X-phase (the gray particles in Fig. 2(b)) is transformed from the dendritical β-$(Mg,Zn)_3Gd$ phase (the white particles in Fig. 2(b)) [12]. The composition is Mg−(8.37±1.0)Zn−(11.32±1.0)Gd (mole fraction, %) and it has a 14H-type LPSO structure like lamellae within matrix. In conclusion, the microstructure of Mg−14.28Gd−2.44Zn−0.54Zr alloy solution-treated at 773 K for 35 h is mainly composed of α-Mg matrix, X-phase at grain boundaries, lamellae within matrix and residual β-$(Mg,Zn)_3Gd$ phase.

3.2 Room-temperature mechanical properties

Figure 3 shows room temperature mechanical properties of the as-cast and solution-treated Mg−14.28Gd−2.44Zn−0.54Zr alloys. The results indicate

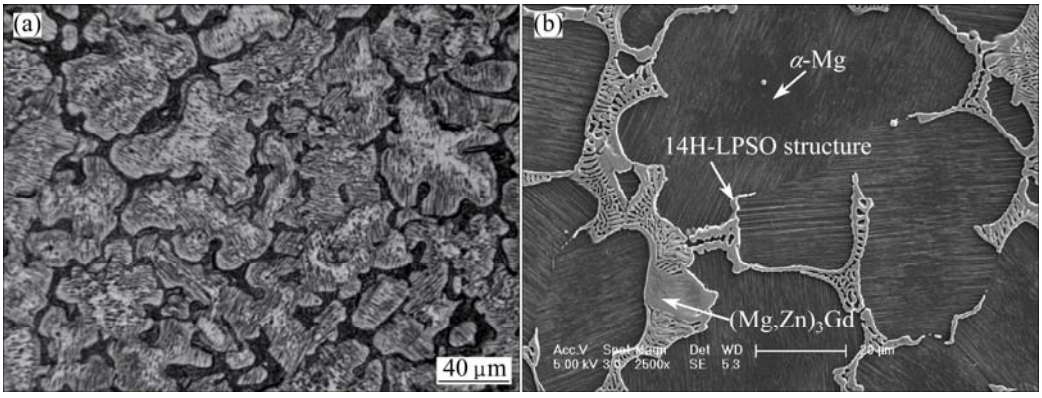

Fig. 1 OM (a) and SEM (b) images of as-cast Mg−14.28Gd−2.44Zn−0.54Zr alloy

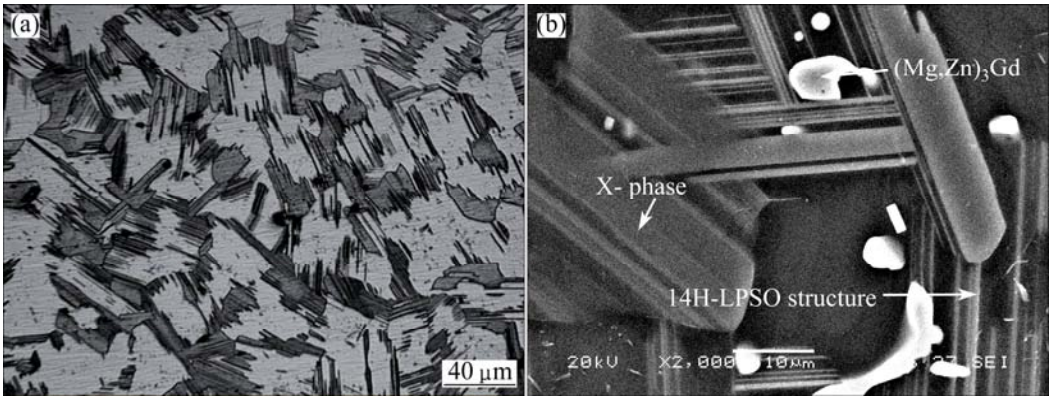

Fig. 2 OM (a) and SEM (b) images of Mg−14.28Gd−2.44Zn− 0.54Zr alloy solution-treated at 773 K for 35 h (T4)

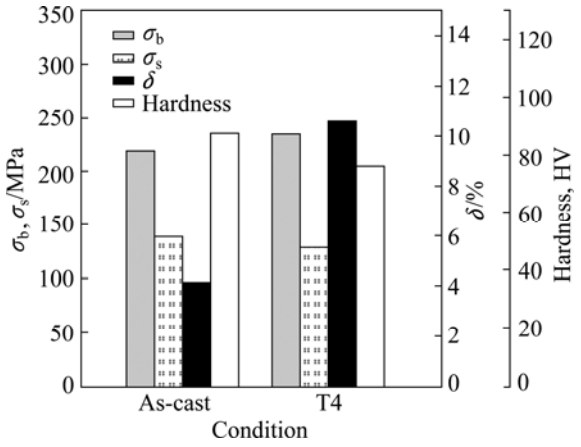

Fig. 3 Room temperature mechanical properties of as-cast and solution-treated Mg−14.28Gd−2.44Zn−0.54Zr alloys

that the comprehensive mechanical properties can be improved after solution heat treatment. The ultimate tensile strength (σ_b) , the tensile yield strength (σ_s), elongations (δ) and Vickers hardness of the as-cast alloy are σ_b=219.9 MPa, σ_s=139.2 MPa, δ=4.2% and HV=87.9, respectively. After solution treatment at 773 K for 35 h, the σ_b and δ are improved to 235.1 MPa and 12.7%, respectively. While, the σ_s and HV decrease to 107.6 MPa and 76.5 due to the reduction of the volume fraction of the harder β-phase and formation of ductile X-phase with 14H-LPSO structure [9].

3.3 Tribological properties

Figure 4 shows variation of friction coefficient (FC) with the sliding time at constant speed of 300 mm/s and load of 40 N for as-cast and solution-treated Mg−14.28Gd−2.44Zn−0.54Zr alloys. It indicates that variation laws of FCs for the as-cast and solution-treated alloys are similar. The FC curves present an initial high friction and then turn into a process of oscillation downward till the steady vibration. However, the average FC values at constant speed of 300 mm/s and load of 40 N are found to be 0.045 and 0.076 for the as-cast and solution-treated alloys, respectively. The FC of solution-treated alloy is clearly higher than that of the as-cast alloy, possibly due to the lower hardness and the higher ductility causing a larger contact area between pin specimen and cast iron.

Figure 5 shows the effects of sliding speed on wear rates of the as-cast and solution-treated Mg−14.28Gd−2.44Zn−0.54Zr alloys. The sliding speeds are 30, 90, 180, 300 mm/s. It shows that the wear rates (W_r) decrease with increasing sliding speed from 30 mm/s to 300 mm/s both in as-cast and solution-treated alloys. Furthermore,

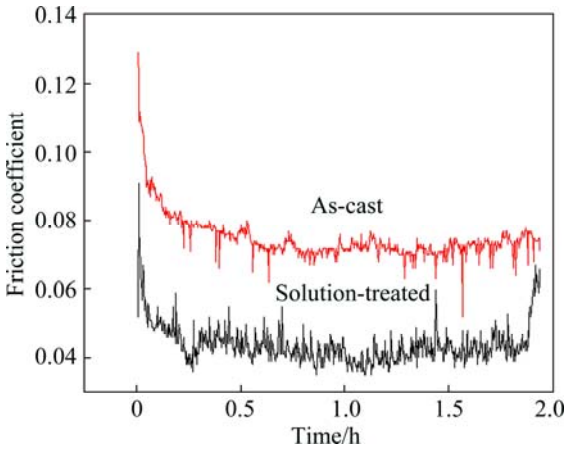

Fig. 4 Variation of friction coefficient with sliding time at constant speed of 300 mm/s and load of 40 N for as-cast and solution-treated Mg−14.28Gd−2.44Zn−0.54Zr alloys

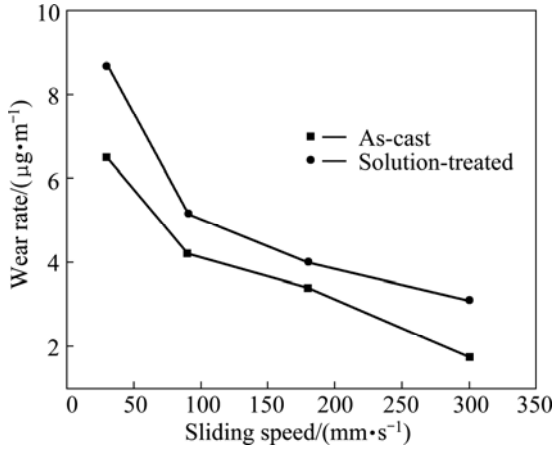

Fig. 5 Effects of sliding speed on wear rate of as-cast and solution-treated Mg−14.28Gd−2.44Zn−0.54Zr alloys

the W_r increases after solution treatment. Generally, the wear rate increases with the increase of the testing load (F_N), as shown in Archard law [21]:

$$W_r=KF_N/H_V \quad (1)$$

where K represents the wear coefficient, and H_V is the microhardness of Mg alloy. As shown in Fig. 3 and Fig. 5, the Vickers hardness of the solution-treated alloy is lower than that of the as-cast alloy, therefore, W_r of the former is higher than that of the latter with the same F_N (40 N). The relative wear resistance can be expressed as the reciprocal of wear rate [22]. In conclusion, the wear resistance of alloy decreases after the solution treatment.

3.4 Analysis of worn surface

Figure 6 shows SEI-SEM and BSE-SEM images of worn surfaces of as-cast Mg−14.28Gd−2.44Zn−0.54Zr alloy at load of 40 N with a sliding distance of 5000 m at sliding speed of 30−300 mm/s. As shown in Figs. 6(a), (b), (d), (e), (g) and (h), numerous long worn grooves parallel to sliding direction are observed. Therefore, the worn surfaces in as-cast Mg−Gd−Zn−Zr alloys exhibit typical features of abrasive wear, which are similar to Mg−Zn−Gd alloys [7]. In the as-cast Mg−Gd−Zn−Zr alloys, WU et al [14] reported that the harder β-$(Mg,Zn)_3Gd$ phases at grain boundaries act as main fracture sources during tensile tests. Abrasive wear is a process wherein the abrasive particles remove from the material by way of cutting or plowing when they slide on the soft material [23]. Therefore, parts of the harder β-phases can be removed from the material resulting in worn grooves during abrasive wear, as shown in Figs. 6(c), (f), (i). Moreover, the β-$(Mg,Zn)_3Gd$ phases are distorted and deformed and broken nearby the worn grooves, which results in the delamination nearby the β-$(Mg,Zn)_3Gd$ phases, due to extrusion and shear effect, as shown in Figs. 6(c) and (f). The grooves become shallower and the surface fracture area decreases with the increase of sliding speed from 30 to 300 mm/s, which results in the wear rate decreasing (see Fig. 5). Meanwhile, it is noted that there is surface oxidation in the form of oxide layer, as shown in Figs. 6(g), (h) and (i), which is attributed to elevated temperature at high sliding speed (300 mm/s). Part of oxide layer being broken on the worn surface is resulted from squeezing and shearing effect in the dynamic load conditions.

Figure 7 shows SEI-SEM and BSE-SEM images of worn surfaces of the Mg−14.28Gd−2.44Zn−0.54Zr alloy solution-treated at 773 K for 35 h at load of 40 N with a sliding distance of 5000 m at sliding speed of 30−300 mm/s. Similar to that of the as-cast alloy, there are some phenomena as follows, as shown in Figs. 7(a), (b), (d), (e), (g) and (h): 1) Numerous long worn grooves parallel to sliding direction are observed; 2) The grooves become shallower and the number of grooves decreases with the increase of sliding speed from 30 mm/s to 300 mm/s, which results in the wear rate decreasing (see Fig. 5); 3) There is surface oxidation in the form of oxide layer (see Fig. 7(h)). Dissimilarly, there are severe plastic deformation (SPD) in ductile X-phase, which will result in the breakup in larger X-phase at last, as shown in Figs. 7(c), (f) and (i). Moreover, little residual β-$(Mg,Zn)_3Gd$ phases appear (see Figs. 7(c), (d) and (i)). Besides the lower hardness and larger contact area, the surface roughness due to tiny and dispersive β-$(Mg,Zn)_3Gd$ phase particles is plausibly responsible for the higher friction coefficient of solution-treated alloy. Delamination occurs in the softer α-Mg matrix (see Fig. 7(h)), and is far away from the harder β-$(Mg,Zn)_3Gd$ phases. The reason that the wear resistance of the Mg−14.28Gd−2.44Zn−0.54Zr alloy decreases after the solution treatment, is mainly due to the obvious decrease of volume fraction of the harder β-phase and formation of ductile X-phase with 14H-LPSO structure.

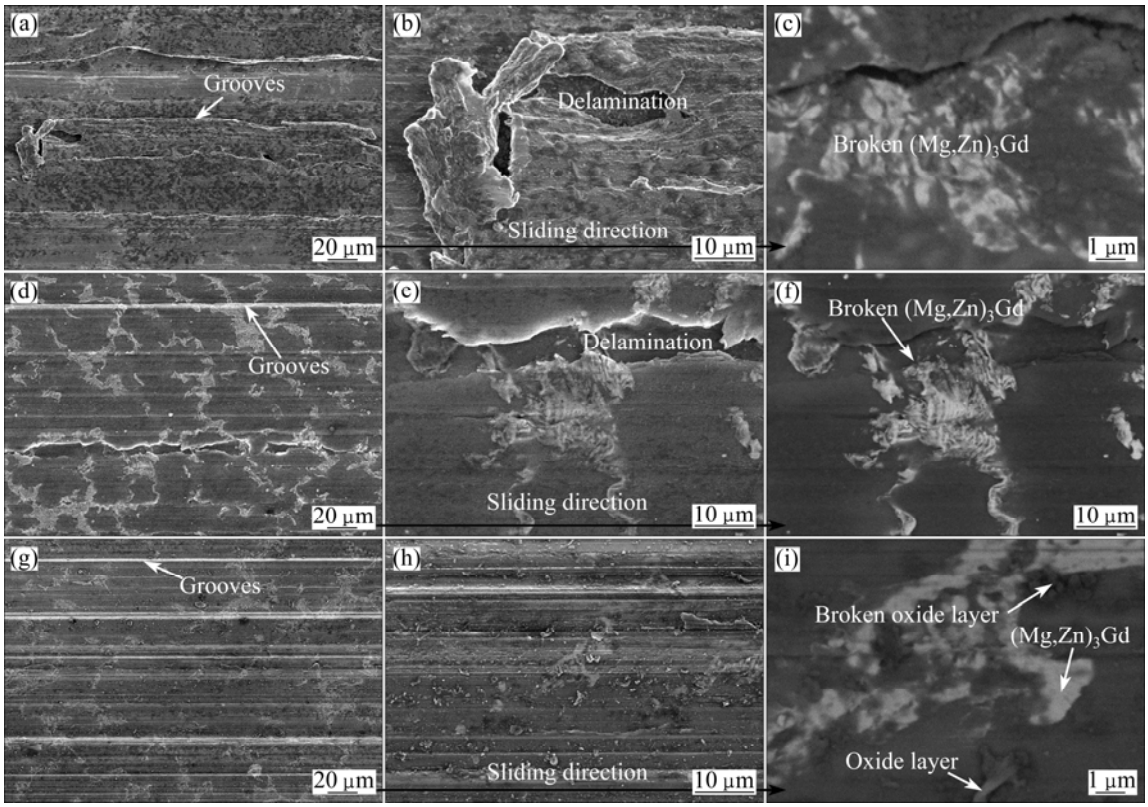

Fig. 6 SEM images of worn surfaces of as-cast Mg−14.28Gd−2.44Zn−0.54Zr alloy at load of 40 N with sliding distance of 5000 m at sliding speed of (a)−(c)30 mm/s, (d)−(f) 180 mm/s and (g)−(i) 300 mm/s ((a),(b),(d),(e).(g),(h) SEI; (c),(f), (i) BSE)

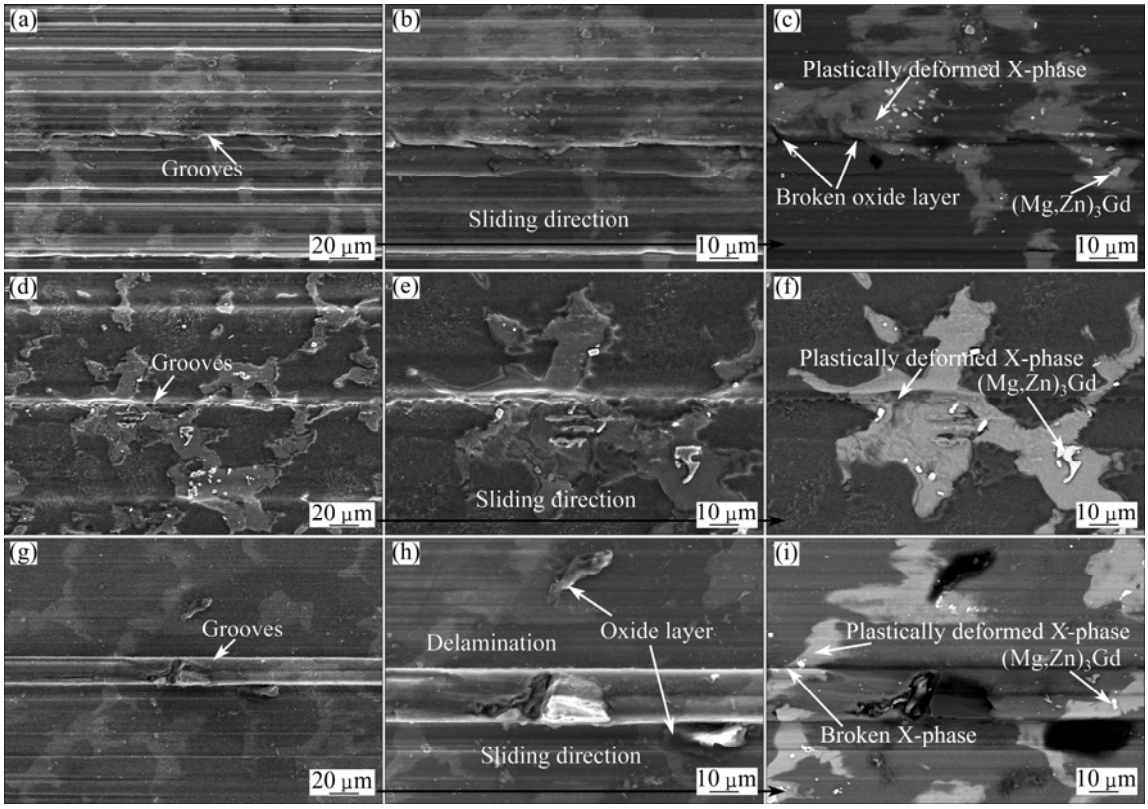

Fig. 7 SEM images of worn surfaces of Mg−14.28Gd−2.44Zn−0.54Zr alloy solution-treated at 773 K for 35 h at load of 40 N with sliding distance of 5000 m at sliding speed of 30 mm/s (a)−(c), 180 mm/s (d)−(f) and 300 mm/s (g)−(i) ((a),(b),(d),(e).(g),(h) SEI;(c),(f), (i) BSE)

4 Conclusions

1) The as-cast Mg−14.28Gd−2.44Zn−0.54Zr alloy is composed of α-Mg solid solution, the lamellar14H-type LPSO structure formed in α-Mg matrix, and β [(Mg,Zn)$_3$Gd] phase as secondary eutectic phase. The microstructure of the Mg−14.28Gd−2.44Zn−0.54Zr alloy solution-treated at 773 K for 35 h is confirmed to be composed of α-Mg matrix, X-phase at grain boundaries, lamellae within matrix and residual (Mg,Zn)$_3$Gd phase.

2) The solution-treated Mg−14.28Gd−2.44Zn−0.54Zr alloy emerges high friction coefficient and wear rate, compared with the as-cast alloy. With the increase of sliding speed from 30 to 300 mm/s, the wear rate decreases for both alloys.

3) Both of the worn surfaces of the as-cast and solution-treated Mg−14.28Gd−2.44Zn−0.54Zr alloys exhibit typical feature of abrasive wear with grooves.

4) The wear resistance of alloy decreases after the solution treatment, due to the obvious decrease of the volume fraction of the harder β-phase and formation of ductile X-phase with 14H-LPSO structure.

References

[1] KULEKCI M K. Magnesium and its alloys applications in automotive industry [J]. International Journal of Advanced Manufacturing Technolog, 2008, 39(9−10): 851−865.

[2] WANG Jing-feng , LU Ruo-peng , WEI Wen-wen , HUANG Xue-fei, PAN Fu-sheng. Effect of long period stacking ordered (LPSO) structure on the damping capacities of Mg–Cu–Mn–Zn–Y alloys [J]. Journal of Alloys and Compounds, 2012, 537: 1−5.

[3] XIE Zhi-wen , LUO Zhuang-zhu, YANG Qin , CHEN Tian , TAN Sheng, WANG Yun-jiao , LUO Yi-min. Improving anti-wear and anti-corrosion properties of AM60 magnesium alloy by ion implantation and Al/AlN/Cr AlN/CrN/MoS_2 gradient duplex coating [J]. Vacuum, 2014, 101: 171−176.

[4] TALTAVULL C, LÓPEZ A J, TORRES B, RAMS J. Dry sliding wear behaviour of laser surface melting treated AM60B magnesium alloy[J]. Surface and Coatings Technology, 2013, 236: 368−379.

[5] LÓPEZ A J, TORRES B, TALTAVULL C, RAMS J. Influence of high velocity oxygen-fuel spraying parameters on the wear resistance of Al–SiC composite coatings deposited on ZE41A magnesium alloy [J]. Materials and Design, 2013, 43: 144−152.

[6] AMANOV AUEZHAN, PENKOV OLEKSIY V, PYUN Y S, KIM D E. Effects of ultrasonic nanocrystalline surface modification on the tribological properties of AZ91D magnesium alloy[J]. Tribology International, 2012, 54: 106−113.

[7] LIU Yong , SHAO Shuang , XU Chun-shui , YANG Xiang-jie , LU De-ping. Enhancing wear resistance of Mg−Zn−Gd alloy by cryogenic treatment [J]. Materials Letters, 2012,76: 201−204.

[8] KAWAMURA Y, HAYASHI K, INOUE A, MASUMOTO T. Rapidly solidified powder metallurgy $Mg_{97}Zn_1Y_2$ alloys with excellent tensile yield strength above 600 MPa [J]. Materials Transactions, 2001, 42(7): 1172−1176.

[9] WU Yu-juan, PENG Li-ming, LIN Dong-liang, DING Wen-jiang. A high-strength extruded Mg−Gd−Zn−Zr alloy with superplasticity [J]. Journal of Materials Research, 2009, 24(12): 596−602.

[10] KAWAMURA Y, YAMASAKI M. Formation and mechanical properties of $Mg_{97}Zn_1RE_2$ alloys with long-period stacking ordered structure [J]. Materials Transactions, 2007, 48(11): 2986−2992.

[11] HAGIHARA K, KINOSHITA A, SUGINO Y, YAMASAKI M, KAWAMURA Y, YASUDA H Y, UMAKOSHI Y. Effect of long-period stacking ordered phase on mechanical properties of $Mg_{97}Zn_1Y_2$ extruded alloy [J]. Acta Materialia, 2010, 58(19): 6282−6293.

[12] ITOI T, SEIMIYA T, KAWAMURA Y, HIROHASHI M. Long period stacking structures observed in $Mg_{97}Zn_1Y_2$ alloy [J]. Scripta Materialia, 2004, 51(2): 107−111.

[13] WU Yu-juan, ZENG Xiao-qin, LIN Dong-liang, PENG Li-ming, DING Wen-jiang. The microstructure evolution with lamellar 14H-type LPSO structure in an $Mg_{96.5}Gd_{2.5}Zn_1$ alloy during solid solution heat treatment at 773K [J]. Journal of Alloys and Compounds, 2009, 477(1−2): 193−197.

[14] WU Yu-juan, LIN Dong-liang, ZENG Xiao-qin, PENG Li-ming, DING Wen-jiang. Formation of a lamellar 14H-type long period stacking ordered structure in an as-cast Mg−Gd−Zn−Zr alloy [J]. Journal of Materials Science, 2009, 44(6): 1607−1612.

[15] DING Wen-jiang, WU Yu-juan, PENG Li-ming, ZENG Xiao-qin, YUAN Guang-yin, LIN Dong-liang.Formation of 14H-type long period stacking ordered structure in the as-cast and solid solution treated Mg–Gd–Zn–Zr alloys [J]. Journal of Materials Research, 2009, 24(5): 1842−1854.

[16] ZENG Xiao-qin, WU Yu-juan, PENG Li-ming, LIN Dong-liang, DING Wen-jiang, PENG Ying-hong. LPSO structure and aging phases in Mg–Gd–Zn–Zr alloy[J]. Acta Metallurgica Sinica, 2010,46(9): 1041−1046. (in Chinese)

[17] HU Mao-liang, WANG Qu-dong, LI Cheng, DING Wen-jiang. Dry sliding wear behavior of cast Mg–11Y–5Gd–-2Zn magnesium alloy [J]. Transactions of Nonferrous Metals Society of China, 2012, 22(8): 1918−1923.

[18] CAO Li-jie, WANG Qu-dong, WU Yu-juan, YE Bing. Friction and wear behavior of Mg–11Y–5Gd–2Zn–0.5Zr (wt%) alloy with oil lubricant [J]. Rare Metals, 2013, 32(5): 453−458.

[19] AN J, LI R G, LU Y, CHEN C M, XU Y, CHEN X, WANG LM. Dry sliding wear behavior of magnesium alloys [J]. Wear, 2008, 265: 97−104.

[20] ZHANG Ying-bo, YU Si-rong, LUO Yan-ru , HU Hai-xia. Friction and wear behavior of as-cast Mg–Zn–Y quasicrystal materials [J]. Materials Science and Engineering A, 2008, 472: 59−65.

[21] ARCHARD J F. Contact and rubbing of flat surfaces [J]. Journal of Applied Physics, 1953, 24: 981−988.

[22] SUN Guo-jin , WU Su-jun, SU Guang-cai. Research on impact wear resistance of in situ reaction TiC_p/Fe composite [J]. Wear, 2010, 269(3−4): 285−290.

[23] PRASAD B K, DAS S, JHA A K, MODI O P, DASGUPTA R, YEGNESWARAN A H. Factors controlling the abrasive wear response of a zinc-based alloy silicon carbide particle composites [J]. Composites, Part A, 1997, 28: 301−308.

具有长周期结构的 Mg–Gd–Zn–Zr 合金的微结构和摩擦学行为

曹丽杰[1]，吴玉娟[2]，彭立明[2]，王渠东[2]，丁文江[2]

1. 上海工程技术大学 机械工程学院，上海 201600；
2. 上海交通大学 轻合金精密成型国家工程研究中心，上海 200240；
3. 上海交通大学 金属基复合材料国家重点实验室，上海 200240；

摘 要：利用传统的熔铸法制备 Mg−14.28Gd−2.44Zn−0.54Zr 合金，研究铸态和固溶态合金的微结构。利用销−盘装置研究铸态和固溶态合金的室温润滑滑动摩擦磨损行为研究。在外载荷为 40 N，滑动速度为 30~300 mm/s 以及滑行路程为 5000 m 情况下，测量磨损率和摩擦因数。研究结果表明：铸态合金主要由 α-Mg 固溶体、分布在基体内的层片状的 14H 型长周期结构(LPSO)和 β-[$(Mg,Zn)_3Gd$]相组成。经过温度为 773 K 固溶处理 35 h 后，大量的 β 相转变成具有 14H 型 X 相 LPSO 结构。由于固溶处理后大量 β 相转变为热稳定的韧性 X-$Mg_{12}GdZn$ 长周期结构相，固溶合金呈现较低的抗磨损能力。

关键词：Mg−14.28Gd−2.44Zn−0.54Zr 合金；长周期结构；微结构；摩擦；磨损

(Edited by Yun-bin HE)